Int J Theor Phys (2010) 49: 1222–1231
DOI 10.1007/s10773-010-0302-9

Quintom Wormholes

Peter K.F. Kuhfittig · Farook Rahaman · Ashis Ghosh

Received: 14 December 2009 / Accepted: 1 March 2010 / Published online: 17 March 2010

Abstract The combination of quintessence and phantom energy in a joint model is referred to as quintom dark energy. This paper discusses traversable wormholes supported by such quintom matter. Two particular solutions are explored, a constant redshift function and a specific shape function. Both isotropic and anisotropic pressures are considered.

Keywords Traversable wormholes · Quintom dark energy · Quintessence · Phantom energy

1 Introduction

A stationary spherically symmetric wormhole may be defined as a handle or tunnel in a multiply-connected spacetime joining widely separated regions of the same spacetime or of different spacetimes [1]. Interest in wormholes was renewed by the realization that much of our Universe is pervaded by a dynamic dark energy that causes the Universe to accelerate [2, 3]: $\ddot{a}$ is positive in the Friedmann equation $\ddot{a}/a = -\frac{4\pi G}{3}(\rho + 3p)$. In the equation of state (EoS) $p = \omega\rho$, a value of $\omega < -1/3$ is required for an accelerated expansion. The range of values $-1 < \omega < -1/3$ is usually referred to as *quintessence* and the range $\omega < -1$ as *phantom energy*. In the latter case we get $\rho + p < 0$, in violation of the weak energy condition, considered to be a primary prerequisite for the existence of wormholes [4–9]. The special case $\omega = -1$ corresponds to Einstein's cosmological constant. This value is sometimes called the *cosmological constant barrier* or the *phantom divide*.

P.K.F. Kuhfittig
Department of Mathematics, Milwaukee School of Engineering, Milwaukee, WI 53202-3109, USA
e-mail: kuhfitti@msoe.edu

F. Rahaman (✉) · A. Ghosh
Department of Mathematics, Jadavpur University, Kolkata 700032, India
e-mail: farook_rahaman@yahoo.com

A. Ghosh
e-mail: ashis_laru@yahoo.co.in

The quintessence and phantom energy models taken together as a *joint model* and dubbed *quintom* for short [10] suggests a single EoS, $p = \omega\rho$, to cover all cases. It is shown in [11], however, that ω cannot cross the phantom divide, that is, in the traditional scalar field model, the EoS cannot cross the cosmological constant barrier. (For further discussion, see [12–16].) The simplest quintom model involves two scalar fields, ϕ and ψ, one quintessence-like and one phantom-like [17, 18]:

$$\mathcal{L} = \frac{1}{2}\partial_\mu\phi\partial^\mu\phi - \frac{1}{2}\partial_\mu\psi\partial^\mu\psi - V(\phi) - W(\psi).$$

So instead of ω in the EoS, we will use ω_q and ω_{ph}, respectively.

One reason for studying quintom dark energy is the bouncing universe [17, 19, 20], which provides a possible solution to the Big-Bang singularity. An extension to the braneworld scenario is discussed in [21].

The purpose of this paper is to study various wormhole spacetimes that are supported by quintom dark energy. We discuss the structure of such wormholes by means of an embedding diagram, as well as the junction to an external Schwarzschild spacetime. Both isotropic and anisotropic pressures are considered. It is shown that in the isotropic models, the phantom-energy condition $\omega_{ph} < -1$ implies that $\omega_q < -1$, while in the anisotropic case, $\omega_q < -1/3$.

As a final comment, since quintessence satisfies the weak and null energy conditions, it is not feasible to model a wormhole using the quintessence field. So when considered as separate fields, only phantom energy can support a wormhole structure.

2 Construction of Quintom Wormholes

In the present study the metric for a static spherically symmetric wormhole spacetime is taken as

$$ds^2 = -e^{\nu(r)}dt^2 + e^{\lambda(r)}dr^2 + r^2(d\theta^2 + \sin^2\theta d\phi^2), \tag{1}$$

where $\nu(r)$ and $\lambda(r)$ are functions of the radial coordinate r.

Let us now consider a quintom model, which, as noted earlier, contains a quintessence-like field and a phantom-like field. So we assume that the Einstein field equations can be written as

$$G_{\mu\nu} = 8\pi G(T_{\mu\nu} + \tau_{\mu\nu}), \tag{2}$$

where $\tau_{\mu\nu}$ is the energy-momentum tensor of the quintessence-like field and is characterized by a free parameter ω_q, which is ordinarily restricted by the condition $\omega_q < -\frac{1}{3}$. (Recall that this condition is required for an accelerated expansion.) According to Kiselev [22], the components of this tensor need to satisfy the conditions of additivity and linearity. Taking into account the different signatures used in the line elements, the components can be stated as follows:

$$\tau_t^t = \tau_r^r = -\rho_q, \tag{3}$$

$$\tau_\theta^\theta = \tau_\phi^\phi = \frac{1}{2}(3\omega_q + 1)\rho_q. \tag{4}$$

The energy-momentum tensor compatible with spherically symmetry is

$$T^{\mu\nu} = (\rho + p)u^\mu u^\nu + pg^{\mu\nu}. \tag{5}$$

As already noted, a phantom-like field is characterized by the equation of state

$$p_r = \omega_{ph}\rho, \tag{6}$$

where p_r is the radial pressure and $\omega_{ph} < -1$. In the discussion below, p_t is the lateral pressure.

The Einstein field equations in the orthonormal frame are stated next:

$$e^{-\lambda}\left[\frac{\lambda'}{r} - \frac{1}{r^2}\right] + \frac{1}{r^2} = 8\pi G(\rho + \rho_q), \tag{7}$$

$$e^{-\lambda}\left[\frac{1}{r^2} + \frac{\nu'}{r}\right] - \frac{1}{r^2} = 8\pi G(p_r - \rho_q), \tag{8}$$

$$\frac{1}{2}e^{-\lambda}\left[\frac{1}{2}(\nu')^2 + \nu'' - \frac{1}{2}\lambda'\nu' + \frac{1}{r}(\nu' - \lambda')\right] = 8\pi G\left(p_t + \frac{(3\omega_q + 1)}{2}\rho_q\right). \tag{9}$$

3 Model 1: A Constant Redshift Function

For our first model we assume a constant redshift function,

$$\nu(r) \equiv \nu_o = \text{constant}, \tag{10}$$

referred to as the zero-tidal-force solution in [1]. The absence of tidal forces automatically satisfies a key traversability criterion.

3.1 Isotropic Pressure

Our first assumption in the present model is an isotropic pressure:

$$p = p_r = p_t.$$

Adding (7) and (8) and using (6) and (10), we get

$$e^{-\lambda}\left[\frac{\lambda'}{r}\right] = 8\pi G(\omega_{ph} + 1)\rho. \tag{11}$$

Multiplying (8) by $(3\omega_q + 1)/2$ and adding to (9) leads to

$$(e^{-\lambda})' + \frac{A_1 e^{-\lambda}}{r} = \frac{A_1}{r}, \tag{12}$$

where

$$A_1 = \frac{(3\omega_q + 1)(\omega_{ph} + 1)}{(\omega_{ph} + 1) + 3\omega_{ph}(\omega_q + 1)}. \tag{13}$$

The above equation yields

$$e^{-\lambda} = 1 - \frac{D}{r^{A_1}}, \tag{14}$$

where $D > 0$ is an integration constant. We rewrite the metric in the Morris-Thorne canonical form [1], $e^{\lambda} = 1/[1 - b(r)/r]$, where the shape function is given by

$$b(r) = \frac{D}{r^{A_1 - 1}}. \tag{15}$$

Using (7) and (8), one gets the following forms for ρ and ρ_q:

$$8\pi G\rho = -\frac{DA_1}{(1+\omega_{ph})r^{A_1+2}} \tag{16}$$

and

$$8\pi G\rho_q = \frac{D(-A_1 + 1 + A_1/(1+\omega_{ph}))}{r^{A_1+2}}. \tag{17}$$

Observe that $\rho > 0$, since $1 + \omega_{ph} < 0$, while $\rho_q > 0$ implies that $A_1 < (1+\omega_{ph})/\omega_{ph}$. It follows that $A_1 < 1$.

The assumption $v(r) \equiv v_0$ implies the absence of a horizon. Also, we would like the wormhole spacetime to be asymptotically flat, that is, $b(r)/r \to 0$ as $r \to \infty$. To this end, we require that $A_1 > 0$. From (13) we deduce that

$$\omega_q < \frac{-4\omega_{ph} - 1}{3\omega_{ph}}.$$

Since $\omega_{ph} < -1$, it now follows that $\omega_q < -1$, thereby having crossed the phantom divide. This result is hardly surprising, given the nature of phantom wormholes. On the other hand, the quintessence condition $\omega_q < -1/3$ is still going to occur, namely in the anisotropic case, discussed next.

3.2 Anisotropic Pressure

In the case of an anisotropic pressure, the radial and lateral pressures are no longer equal. In an earlier paper on phantom-energy wormholes, Zaslavskii [4] proposed the form $p_t = \alpha\rho$, $\alpha > 0$, for the lateral pressure. In this manner we obtain simple linear relationships between pressure and energy-density, but with p_r not equal to p_t.

Observe first that (11) remains the same. After multiplying (8) by $(3\omega_q + 1)/2$ and adding to (9), we get, analogously,

$$(e^{-\lambda})' + \frac{A_2 e^{-\lambda}}{r} = \frac{A_2}{r}, \tag{18}$$

where

$$A_2 = \frac{(3\omega_q + 1)(\omega_{ph} + 1)}{(\omega_{ph} + 1) + 2\alpha + \omega_{ph}(3\omega_q + 1)}. \tag{19}$$

Otherwise (14)–(17) retain their form.

As before, we want $A_2 > 0$. So from (19), we have

$$\omega_{ph} + 1 + 2\alpha + \omega_{ph}(3\omega_q + 1) > 0$$

and

$$\omega_q < \frac{-2\omega_{ph} - 1 - 2\alpha}{3\omega_{ph}}. \tag{20}$$

Since $\alpha > 0$ and $\omega_{ph} < -1$, it follows that

$$\omega_q < -\frac{1}{3},$$

which is the condition for quintessence. In other words, in the anisotropic model, ω_q does not have to cross the phantom divide.

Remark The parameter α could be negative. For example, if $\alpha < -1$, we return to $\omega_q < -1$.

4 Wormhole Structure

In this section we let $A = A_i, i = 1, 2$. Returning to the shape function $b(r) = D/r^{A-1}$, to meet the condition $b(r_0) = r_0$, we must have $D = r_0^A$. So the radius of the throat is $r_0 = D^{1/A}$ and

$$b(r) = r\left(\frac{r_0}{r}\right)^A.$$

Since $A > 0$, it now follows that $b'(r_0) < 1$, thereby satisfying the flare-out condition. From [1], we therefore obtain the "exoticity condition"

$$\frac{b(r_0) - r_0 b'(r_0)}{2[b(r_0)]^2} = \frac{A}{2r_0^2} > 0,$$

which shows that the weak energy condition has been violated. We already checked the asymptotic flatness, so that our solution describes a static traversable wormhole supported by quintom dark energy.

As discussed in [1], one can picture the spacial shape of a wormhole by rotating the profile curve $z = z(r)$ about the z-axis. This curve is defined by

$$\frac{dz}{dr} = \pm\frac{1}{\sqrt{r/b(r) - 1}} = \pm\frac{1}{\sqrt{r^A/D - 1}}. \tag{21}$$

For example, choosing $A = \frac{1}{2}$, we find that

$$z = 4\sqrt{D}\left[\frac{1}{3}(\sqrt{r} - D)^{3/2} + D\sqrt{(\sqrt{r} - D)}\right]. \tag{22}$$

The profile curve is shown in Fig. 1 and the embedding diagram in Fig. 2. The proper distance $l(r)$ from the throat to a point outside is given by

$$l(r) = \pm\int_{r_0^+}^{r} \frac{dr}{\sqrt{1 - b(r)/r}}. \tag{23}$$

For $A = \frac{1}{2}$,

$$l(r) = r^{1/4}(\sqrt{r} - D)^{3/2} + \frac{5D}{2}r^{1/4}(\sqrt{r} - D)^{1/2} + \frac{3}{2}D^2\ln\left|\frac{r^{1/4} + (\sqrt{r} - D)^{1/2}}{\sqrt{D}}\right|. \tag{24}$$

(See Fig. 3.)

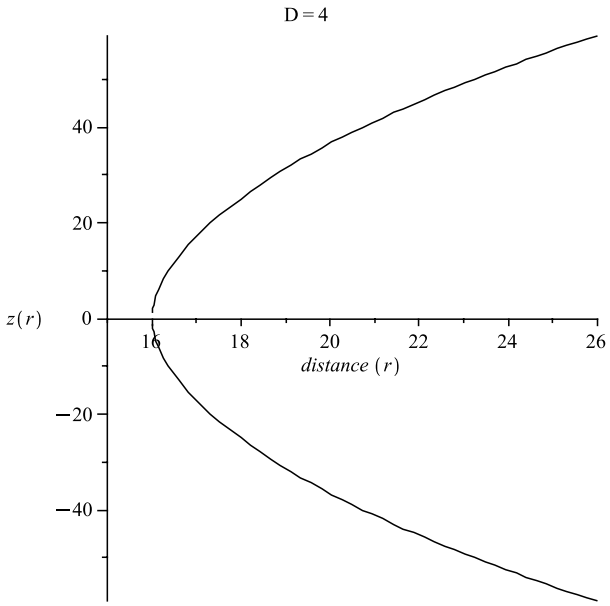

Fig. 1 The profile curve of the wormhole

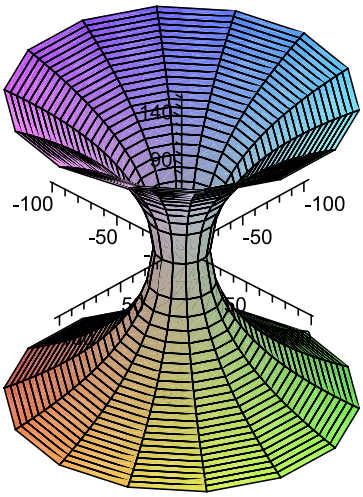

Fig. 2 The embedding diagram generated by rotating the profile curve (Fig. 1) about the z-axis

It is customary to join the interior solution of a wormhole to an exterior Schwarzschild solution at some $r = a$. To do so, we demand that g_{tt} and g_{rr} be continuous at $r = a$:

$$g_{tt\,(int)}(a) = g_{tt\,(ext)}(a)$$

and

$$g_{rr\,(int)}(a) = g_{rr\,(ext)}(a);$$

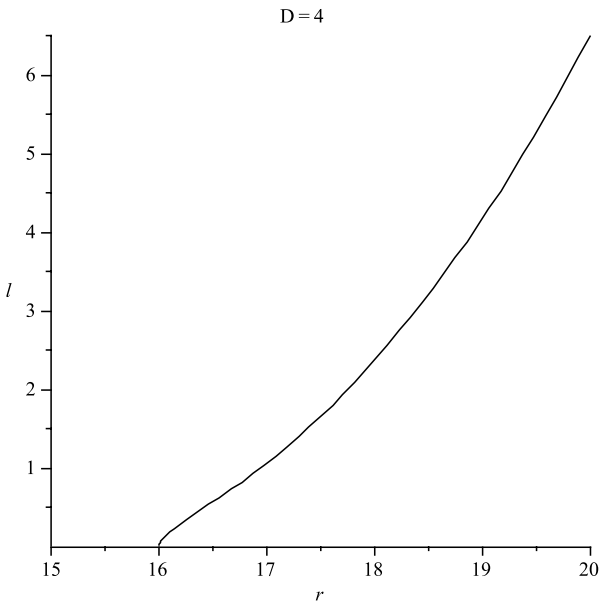

Fig. 3 The graph of the radial proper distance $l(r)$

$g_{\theta\theta}$ and $g_{\phi\phi}$ are already continuous [23]. So $e^{\nu_0} = 1 - \frac{2GM}{a}$ and $1 - \frac{b(a)}{a} = 1 - \frac{2GM}{a}$. This, in turn, implies that $D/a^{A-1} = 2GM$. Hence, the matching occurs at

$$a = \left(\frac{D}{2GM}\right)^{1/(A-1)}. \tag{25}$$

The interior metric ($r_0 < r \leq a$) is given by

$$ds^2 = -\left[1 - \frac{D}{a^A}\right]dt^2 + \frac{dr^2}{1 - D/r^A} + r^2(d\theta^2 + \sin^2\theta d\phi^2) \tag{26}$$

and the exterior metric ($a < r < \infty$) by

$$ds^2 = -\left[1 - \frac{D}{a^{A-1}r}\right]dt^2 + \frac{dr^2}{1 - D/a^{A-1}r} + r^2(d\theta^2 + \sin^2\theta d\phi^2). \tag{27}$$

5 Model 2: A Specific Shape Function

Returning to the isotropic case $p = p_r = p_t$, let us eliminate ρ and ρ_q in (7)–(9) to obtain the following master equation:

$$\frac{1}{4}(\nu')^2 + \frac{1}{2}\nu'' + \nu' g(r) = -\frac{e^{\lambda}}{2r}\frac{(\omega_{ph} + 1) + 3\omega_{ph}(\omega_q + 1)}{\omega_{ph} + 1} f(r), \tag{28}$$

where

$$g(r) = -\frac{\lambda'}{4} + \frac{1}{2r} + \frac{3\omega_q + 1}{2r} - \frac{3\omega_{ph}(\omega_q + 1)}{2(\omega_{ph} + 1)r} \tag{29}$$

and

$$f(r) = (e^{-\lambda})' + \frac{A_1 e^{-\lambda}}{r} - \frac{A_1}{r}. \tag{30}$$

As in (13),

$$A_1 = \frac{(3\omega_q + 1)(\omega_{ph} + 1)}{(\omega_{ph} + 1) + 3\omega_{ph}(\omega_q + 1)}. \tag{31}$$

Now we choose the shape function $b(r)$ in such a way that the right-hand side of (28) is zero. For this specific choice, one gets the following solution:

$$e^{-\lambda} = \frac{1}{1 - b(r)/r} = 1 - \frac{D}{r^{A_1}}, \tag{32}$$

where $D > 0$ is an integration constant. Fortunately, this form is the same as in Model 1. So the physical characteristics, such as the profile curve, the embedding diagram, and the proper radial distance, remain the same. But the redshift function and stress-energy components are different.

By making the proper substitutions, one gets from (28)

$$\nu'' + \frac{\nu'}{r}\left[\frac{A_1 D}{2(r^{A_1} - D)} + L_1\right] = -\frac{(\nu')^2}{2}, \tag{33}$$

where

$$L_1 = (3\omega_q + 2) - \frac{3\omega_{ph}(\omega_q + 1)}{(\omega_{ph} + 1)}. \tag{34}$$

Solving this equation, we get

$$\nu = \ln\left[E D A_1 + \sqrt{1 - \frac{D}{r^{A_1}}}\right]^2, \tag{35}$$

where E is an integration constant. We have used the condition $L_1 = A_1 + 1$. Starting with $L_1 - 1 = A_1$ and simplifying, one can readily deduce that $\omega_q = \omega_{ph}$; so once again, $\omega_q < -1$, thereby having crossed the phantom divide. This is consistent with the isotropic case discussed in Sect. 3.1. (There is a similar consistency with the anisotropic case, as shown at the end of the present section.)

Finally, we get the following forms for ρ and ρ_q:

$$8\pi G\rho = -\frac{D A_1}{(1 + \omega_{ph}) r^{A_1 + 2}}\left[\frac{A_1 D E r^{A_1/2}}{\sqrt{(r^{A_1} - D)} + A_1 D E r^{A_1/2}}\right] \tag{36}$$

and

$$8\pi G\rho_q = \frac{D(-A_1 + 1)}{r^{A_1+2}} + \frac{D A_1}{(1 + \omega_{ph}) r^{A_1+2}}\left[\frac{A_1 D E r^{A_1/2}}{\sqrt{(r^{A_1} - D)} + A_1 D E r^{A_1/2}}\right]. \tag{37}$$

In the anisotropic case $p_t = \alpha\rho$, $\alpha > 0$, eliminating ρ and ρ_q in (7)–(9) yields

$$\frac{1}{4}(\nu')^2 + \frac{1}{2}\nu'' + \nu' g(r) = -\frac{e^{-\lambda}}{2r}\frac{(\omega_{ph} + 1) + 2\alpha + \omega_{ph}(3\omega_q + 1)}{\omega_{ph} + 1} f(r), \tag{38}$$

where

$$g(r) = -\frac{1}{4}\lambda' + \frac{1}{2r} + \frac{3\omega_q + 1}{2r} - \frac{\omega_{ph}(3\omega_q + 1) + 2\alpha}{2(\omega_{ph} + 1)r} \tag{39}$$

and

$$f(r) = (e^{-\lambda})' + \frac{A_2 e^{-\lambda}}{r} - \frac{A_2}{r}; \tag{40}$$

here A_2 is defined in (19). In (33), A_1 is replaced by A_2 and L_1 by

$$L_2 = 1 + (3\omega_q + 1) - \frac{\omega_{ph}(3\omega_q + 1) + 2\alpha}{\omega_{ph} + 1}. \tag{41}$$

From the condition $L_2 - 1 = A_2$, we deduce that

$$\omega_q = \frac{\omega_{ph} + 2\alpha}{3}.$$

Since $\omega_{ph} < -1$ and $\alpha > 0$, we obtain, once again,

$$\omega_q < -\frac{1}{3}.$$

6 Discussion

The combination of quintessence and phantom energy in a joint model is referred to as quintom dark energy. The quintessence-like field is characterized by a free parameter ω_q with the restriction $\omega_q < -1/3$. For the corresponding free parameter ω_{ph} in the phantom-like field, the condition is $\omega_{ph} < -1$.

We have proposed in this paper that traversable wormholes may be supported by quintom dark energy. Two models were considered. The first model, a constant redshift function, leads to the determination of the shape function $b = b(r)$, which meets the flare-out conditions. The resulting spacetime is asymptotically flat. This was followed by a brief discussion of the wormhole structure, including an embedding diagram, proper distance, and a junction to an external Schwarzschild spacetime. For the second, more general model, it is possible to use the same shape function but with a different redshift function and stress-energy components.

In each of these models, both isotropic and anisotropic pressures were considered. In the isotropic case, the phantom-energy condition $\omega_{ph} < -1$ implies that $\omega_q < -1$, and in the anisotropic case, $\omega_{ph} < -1$ implies that $\omega_q < -1/3$.

Acknowledgements FR wishes to thank UGC, Government of India, for providing financial support. FR is also grateful for the research facilities provided by IMSc.

References

1. Morris, M.S., Thorne, K.S.: Am. J. Phys. **56**, 395 (1988)
2. Riess, A.G., et al.: Astron. J. **116**, 1009 (1998)
3. Perlmutter, S.J., et al.: Astrophys. J. **517**, 565 (1999)
4. Zaslavskii, O.B.: Phys. Rev. D **72**, 061303 (2005)

5. Lobo, F.S.N.: Phys. Rev. D **71**, 084011 (2005)
6. Kuhfittig, P.K.F.: Class. Quantum Gravity **23**, 5853 (2006)
7. Rahaman, F., et al.: Phys. Lett. B **633**, 161 (2006)
8. Rahaman, F., et al.: Phys. Scr. **76**, 56 (2007)
9. Rahaman, F., et al.: Gen. Relativ. Gravit. **39**, 145 (2007)
10. Feng, B., Wang, X., Zhang, X.: Phys. Lett. B **607**, 35 (2005)
11. Xia, J.-Q., Cai, Y.-F., Qiu, T.-T., Zhao, G.-B., Zhang, X.-M.: arXiv:astro-ph/0703202
12. Zhao, G.-B., Xia, J.-Q., Li, M., Feng, B., Zhang, X.: Phys. Rev. D **72**, 123515 (2005)
13. Caldwell, R.R., Doran, M.: Phys. Rev. D **72**, 043527 (2005)
14. Vikman, A.: Phys. Rev. D **71**, 023515 (2005)
15. Hu, W.: Phys. Rev. D **71**, 047301 (2005)
16. Kunz, M., Sapone, D.: Phys. Rev. D **74**, 123503 (2006)
17. Cai, Y.-F., Qiu, T., Brandenberger, R., Piao, Y.-S., Zhang, X.: J. Cosmol. Astropart. Phys. **0803**, 013 (2008)
18. Guo, Z.-K., Piao, Y.-S., Zhang, X., Zhang, Y.-Z.: Phys. Lett. B **608**, 177 (2005)
19. Cai, Y.-F., Qiu, T., Piao, Y.-S., Li, M., Zhang, X.: J. High Energy Phys. **0710**, 071 (2007)
20. Zhao, W., Zhang, Y.: Phys. Rev. D **73**, 123509 (2006)
21. Moyassari, P., Setare, M.R.: Phys. Lett. B **674**, 237 (2009)
22. Kiselev, V.V.: Class. Quantum. Gravity **20**, 1187 (2003)
23. Lemos, J.P.S., Lobo, F.S.N., de Oliveira, S.Q.: Phys. Rev. D **68**, 064004 (2003)